

Femi Philip and Samir R. Kapadia

Introduction

Coronary artery disease remains the leading cause of death in the United States and an estimated 1.4 million Americans have a heart attack every year [1]. Coronary atherosclerosis starts at a young age but the initial plaque does not encroach on the lumen but remodeling of the vessel wall occurs by expansion of the external elastic lamina—a phenomenon described by Glagov as positive remodeling [2]. Coronary angiography visualizes the vessel lumen but does not provide any information about the individual components of the vessel wall. Despite this limitation, coronary angiography is the most common method used to delineate the extent and severity of atherosclerotic narrowing of coronary arteries. This modality provides a two dimensional rendering of a three dimensional structure and is dependent on angle of visualization and morphology of lesions visualized. Intravascular techniques using intravascular ultrasound (IVUS) and optical coherence tomography (OCT) provide information complementary to that provided by conventional coronary angiography. This chapter will discuss the technical aspects of these imaging techniques and provide some insights in their clinical applications.

F. Philip, MD • S.R. Kapadia, MD (✉)
Department of Cardiovascular Medicine, Cleveland
Clinic, 9500 Euclid Avenue, Cleveland, OH 44195, USA
e-mail: kapadia@ccf.org

Normal arterial walls consist of an inner layer called the intima, a middle muscular layer called the media and an outermost layer called the adventitia. The intima is the inner most lining of the vessel wall and is in direct contact with components of blood and is normally 1–2 layers thick (varies with the extent of atherosclerotic plaque) and is separated from the media by an inner elastic lamina. The media is the middle layer of the arterial wall and consists predominantly of smooth muscle cells and is separated from the adventitia by an external elastic lamina. The adventitia surrounds the media and is composed of fibrous connective tissue and provides the majority of the external support for the vessel.

Intravascular Ultrasound

IVUS allows visualization of the coronary arterial wall by utilizing a miniature transducer mounted on a flexible catheter that transmits ultrasound in the 10–40 megahertz (MHz) range [3]. Currently, IVUS transducers are oriented at 90° to the length of the catheter to produce a cross-sectional view of the coronary artery. There are currently two types of IVUS catheters in use today: mechanical and phased array.

- Mechanical catheters utilize a single mechanical transducer mounted on a catheter tip that rotates to visualize the entire vessel wall in cross-section. The design is simple with a high signal to power output and produces excellent overall resolution of up to 100–150

micrometers (μm). The images are dependent upon uniform rotation of the transducer and are difficult to use in tortuous vessels.

- Phased array catheters use multiple transducer elements that are mounted on the circumference of the catheter tip. Each of these elements sends and receives ultrasounds from a sector that corresponds to a portion of the vessel wall. When these images are incorporated, they produce a cross-sectional image of the vessel wall. Image resolution is somewhat less than mechanical catheters especially close to the transducer, but the ease of use of these catheters has made them very popular.

Components of the IVUS Image

The cross-sectional image of the arterial wall that is obtained occurs as a result of differential tissue acoustic impedance to ultrasound. The IVUS catheter emits ultrasound waves from the catheter tip and these waves will be reflected back as it encounters an interface of different acoustic impedance. Acoustic impedance is primarily dependent upon the density of the tissue. Therefore, ultrasound will traverse blood with minimal reflection and be highly reflected as it encounters the intima. These reflected ultrasound waves would be displayed as a single concentric echo. Some of the ultrasound will not be reflected and will penetrate into the media. Since the media is composed of smooth muscle cells, ultrasound will pass through with minimal reflection and will appear as a dark zone. The remainder of the ultrasound waves will penetrate and encounter the adventitia and will be highly reflected due to the presence of dense collagen fibers. In essence the normal arterial wall will consist of a series of alternating bright and dark echoes called the normal “three layer appearance” of the coronary artery [4–6]. This is not strictly correct since IVUS resolution is approximately $\sim 120\ \mu\text{m}$ and is not able to detect a truly normal endothelial layer (thickness of $50\ \mu\text{m}$) seen in Fig. 2.3. However, this inner layer becomes quite well visualized in the presence of atherosclerotic disease. Therefore, IVUS images are able to delineate the

extent, morphology, and distribution of atherosclerotic plaque (concentric versus eccentric plaque distribution). This makes IVUS uniquely suited for determining severity of an eccentric plaque over conventional angiography where this can be more challenging as shown in Fig. 2.1. In addition, due to the high resolution of IVUS, vessel wall and plaque size can be more precisely quantified. While angiography allows measurement of luminal diameters in 2 or 3 orthogonal views, IVUS extends this by providing a 360° tomographic view allowing a precise assessment of vessel size. The true maximal and minimal luminal diameter (MLD) can be obtained by IVUS with cross-sectional area measurements of both the lumen and the vessel [6–10].

Information regarding plaque composition is also available with the use of IVUS, as different plaque compositions will reflect ultrasound differently. The characteristic architecture of a thin-cap fibroatheromas (TCFA) overlying a lipid pool has prompted enhancements in IVUS, including backscatter-intravascular ultrasound (BS-IVUS), virtual histology-intravascular ultrasound (VH-IVUS), IVUS elastography, and palpography. Conventional gray-scale angiography is limited in its ability to characterize plaque components. Automatic processing uses the amplitude of the backscattered echo signal to differentiate highly echogenic components (calcium and fibrous tissues) from echolucent ones (lipid and necrotic cores) but it is not able to accurately distinguish between fibrous from fatty plaques [11]. Virtual histology IVUS uses an autoregression model to generate multiple spectral parameters of the backscattered ultrasound signal. These parameters are used in classification of trees to generate a tissue map of the plaque components: fibrous (dark green), fibrofatty (yellow-green), necrotic core (red), and dense calcium (white). The VH-IVUS has been validated in histopathology of autopsy specimens and found to have an accuracy of 79.7, 81.2, and 92.8 % in detecting fibrous, necrotic cores, and calcium, respectively [12, 13]. Backscatter IVUS uses fast Fourier transformation to extract buried frequency components in the original IVUS signal. In autopsy-based studies, the sensitivity of

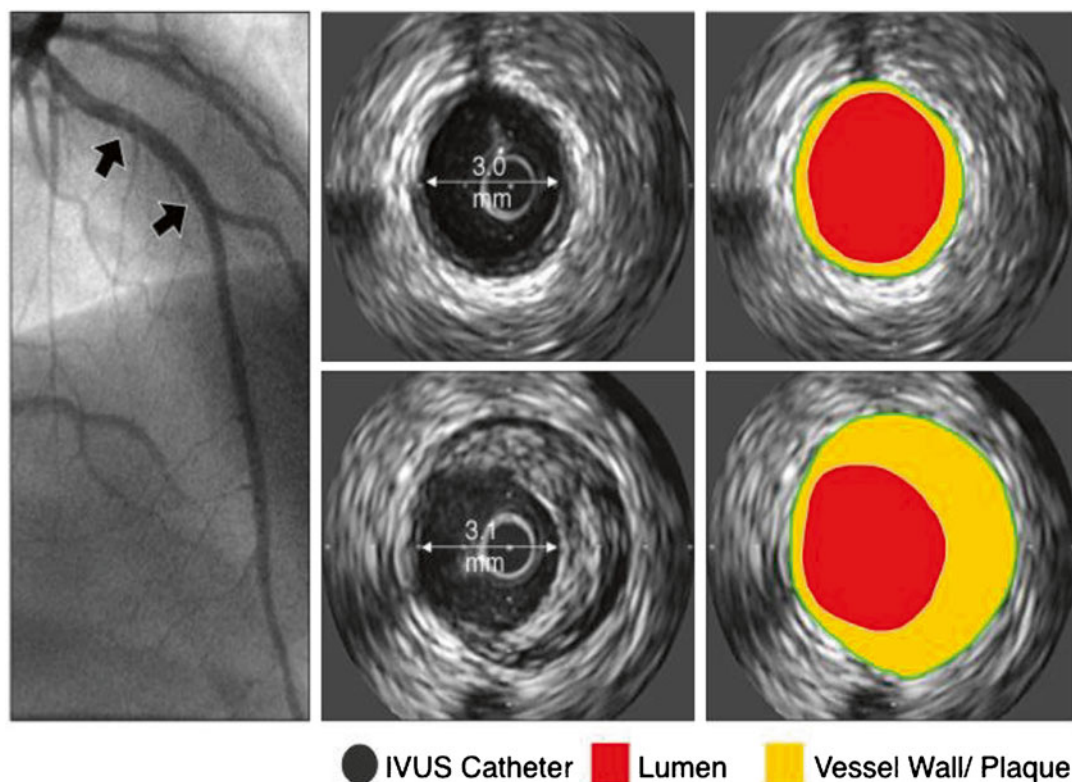


Fig. 2.1 Intravascular ultrasound image of mid-segment of the left anterior descending artery. The *top arrow* coincides with the top two IVUS images and the *lower arrow* with the lower two IVUS images. The atherosclerotic plaques are shown in yellow, vessel lumen in red and

IVUS catheter in gray. In comparison to the accompanying angiogram, the IVUS images show almost half of the vessel area filled by atherosclerotic plaque. The plaque is not associated with luminal stenosis, because it has expanded the vessel size at the lesion site

IB-IVUS for calcification, fibrous and lipid-rich plaque was 100 %, 94 %, and 84 %, respectively, which compares favorably with OCT (100 %, 98 %, and 95 %, respectively) and when compared to “VH-IVUS” there is higher diagnostic accuracy with histological assessments [14]. Intravascular elastography and palpography are methods to assess the strain properties of atherosclerotic coronary arteries using tissue characteristics to determine the degree of deformation of vessel walls [15, 16]. Additional information provided by IVUS has improved our understanding in several areas for example gender-specific differences in atherosclerosis. The coronary vessels in women tend to have a smaller lumen and external elastic lamina in comparison to men [17]. Interestingly these vessel dimensions change in heart transplantation when a donor female heart is transplanted into a male recipient suggesting

some direct hormonal influence. In addition, the extent of atherosclerotic calcification is higher in men than in women suggesting an earlier onset of atherosclerosis with potentially different pathophysiology to injury [18]. These differences may help to understand differences in outcomes of percutaneous coronary intervention (PCI) in women compared to men. In some situations IVUS provides more precise quantification of plaque morphology over conventional coronary angiography. Coronary angiography provides an imprecise measure of lumen morphology and size especially when there is haziness noted in the vessel [19, 20]. This can be due to the presence of irregular plaque, dissection, thrombus, or calcified plaque. IVUS can help to distinguish between these and can often reclassify “angiographically” normal vessels into those with diffuse disease [21].

IVUS provides visualization of vessel wall which is critical to study of plaque and arterial remodeling. The coronary arteries are living structures that can adapt and change with atherosclerosis. Coronary arteries will initially enlarge over time to accommodate focal plaque deposition in an attempt to preserve luminal integrity. This compensatory enlargement to preserve luminal diameter will not be seen on conventional angiography [22–24].

Clinical Applications of IVUS

Anatomically Ambiguous Lesions

IVUS is useful in characterizing angiographically ambiguous lesions including intermediate lesions, ostial stenosis at branch vessels, sites with dissections, and plaque rupture [25]. However, specific threshold criteria for intervention derived by IVUS have not been prospectively validated with noninvasive assessments of myocardial ischemia. Functional lesion assessment using a coronary pressure wire has been prospectively validated and some studies have provided concordance between IVUS characteristics and functional flow reserve (FFR) of <0.75 [26]. The most consistent IVUS cutoff value for major epicardial coronary arteries (excluding the left main) with moderate correlation with an $\text{FFR} < 0.75$ are minimal luminal area (MLA) in the range of 3–4 mm [2]. Furthermore, an MLA of >4 mm [2] is associated with a good clinical outcome but has a low FFR-based specificity. While a combination of an MLA <1.8 mm and angiographic area stenosis of $>70\%$ has a better sensitivity (100 %) [27]. Taken together, these modalities are synergistic and may lead to a reduction of many unnecessary revascularization procedures for intermediate lesions.

Left Main Lesions

The correlation between IVUS measurements and FFR within the epicardial tree is modest. The left main trunk is uniquely suited given the large

vessel size and variable length allows a greater degree of concordance between these two modalities. The MLA of the LMCA on IVUS was a strong predictor of the rate of major adverse cardiac events [28]. Furthermore, several outcome-based studies have addressed the IVUS criteria that correlates with FFR and major adverse cardiovascular events (MACE) but an MLD of 2.8 mm [2] was found to have the highest sensitivity and specificity (93 % and 95 %, respectively) for defining true functional significance of the ULMA stenosis. In the absence of corresponding physiological measurements, IVUS-based criteria of LM compromise have been successfully used to solely guide clinical decision making. While several values have been studied, an MLA of <6 mm [2] has been used as a binary cutoff to defer those who can be managed with revascularization versus medical therapy [29].

Percutaneous Coronary Intervention

The use of IVUS in PCI helps in planning a pre-intervention strategy based on vessel morphology, the presence of calcium, and the burden of thrombus in the vessel and is supported by the American Heart Association (ACC/AHA) PCI guidelines [30]. Adequacy of stent deployment can be very effectively studied with IVUS. Several IVUS characteristics have been associated with increased adverse events after PCI with bare-metal stents (BMS), including smaller minimal stent area (MSA), stent underexpansion, persistent edge dissections, incomplete stent apposition (ISA), and incomplete lesion coverage [31–36]. Smaller MSA has been most commonly associated with target vessel failure at follow-up with rates of restenosis reduced by 19 % per 1 mm [2] increase in MSA [37]. The main clinical benefit of an IVUS-guided BMS PCI strategy is driven by a reduction in restenosis rate and target vessel revascularization (TLR) [38].

There is increasing evidence for utility of an IVUS-directed approach in drug-eluting stenting (DES) [39]. Most of the evidence is however retrospective. Although the randomized trials including HOME-DES (Long-Term Health

Outcome and Mortality Evaluation After Invasive Coronary Treatment Using Drug-Eluting Stents with or without IVUS Guidance) and AVIO (Angiography versus IVUS Optimization) did not demonstrate lower rates of TLR or improved clinical outcomes, IVUS provides important clinical information in many patients to justify its widespread use [40, 41]. There is some evidence for benefit with IVUS-directed DES placement with a reduction in the incidence of stent thrombosis [42], detection of high-grade edge dissections [43] and stent underexpansion [44]. IVUS may also have a role in the treatment of long lesions (>20 mm) which was studied in the TULIP study when at 12 months the use of IVUS guidance was associated with a significant reduction in angiographic restenosis (23 % versus 45 %) and TLR (10 % versus 23 %) [45]. In unprotected left main PCI, the adverse effects of suboptimal stenting are more dramatic and in this subset IVUS guidance is of particular use. This was studied in the MAIN-COMPARE (Revascularization for Unprotected Left Main Coronary Artery Stenosis: Comparison between Percutaneous Coronary Angioplasty Versus Surgical Revascularization) trial. In this analysis, there was a trend toward lower 3-year mortality in the IVUS-guided strategy versus angiography alone group (6.0 % versus 13 % $P=0.0063$) and this was significant in the subgroup receiving DES (4.7 % versus 16 %, $P=0.048$) [40]. IVUS is also advocated by the ACC/AHA PCI guidelines in assisting in the treatment of in-stent restenosis (ISR) [30]. In these cases, IVUS can assist in differentiating between restenosis due to intimal hyperplasia versus that due to mechanical complications such as strut fracture or stent underexpansion.

Allograft Coronary Vasculopathy

Since the intimal and medial layers of the arterial wall have differing acoustical densities, IVUS can distinguish these layers and thereby detect abnormal thickening of the intima. IVUS detects intimal thickening in more than 80 % of patients as early as one year after transplantation. The most rapid

rate of intimal thickening occurs in the first year after transplantation, followed by a slower rate of thickening. This process is diffuse and circumferential, many patients with moderate to severe intimal thickening on IVUS. These changes are not detectable on coronary angiography. The proximal segments of the transplanted coronary arteries have focal and eccentric pattern (similar to that seen in native coronary arteries) while the mid and distal segments of the vessels have diffuse and circumferential disease. This suggests at least two etiologies for the vascular lesions: proximal disease that may be donor-transmitted; and distal disease that may be the result of acquired immune-mediated vessel injury exacerbated by significant metabolic perturbations that occur after transplant. The only possible way to distinguish between donor-transmitted disease and de novo allograft vasculopathy is by performing serial IVUS studies starting with a baseline imaging early after transplant. The identification of allograft vasculopathy has prognostic importance. It has been noted that the absence of angiographic coronary disease was a significant predictor of survival without adverse cardiac events at 2 years [46]. Worsening global TIMI frame count (the mean TIMI FC for the three coronary arteries) from baseline to one year was associated with increased mortality rate during mean 4.3-year follow-up [47–51]. Abnormalities detected by IVUS are predictive of cardiac events and death. In a multicenter study of 125 patients, the change in maximal intimal thickness (MIT) from baseline to 1 year was compared at several matched sites in the same coronary artery. An increase in MIT of ≥ 0.5 mm was present in 24 patients (19 %). At 5-year follow-up, these 24 patients had more frequent death or graft loss (20.8 versus 5.9 % in those with an MIT increase <0.5 mm) [46]. Similar findings were noted in a series of 143 patients in which MIT on IVUS was measured at baseline and 1 year; rapidly progressive vasculopathy was again defined as an increase in MIT of ≥ 0.5 mm [50]. Rapid progression by IVUS was noted in 54 patients (37 %) at 1 year after transplant. At 5.9-year follow-up, patients with rapid progression at 1 year had significantly higher rates of mortality (26 versus 11 % in those with an MIT increase of

less than 0.5 mm), the combined endpoint of death or myocardial infarction (51 versus 16 %), as well as angiographic disease (22 and 2 %).

These data have led to use of IVUS as a surrogate endpoint in clinical trials of new immunosuppressive and other agents known to affect intimal proliferation. Given the cost, small risk and the time-consuming nature of the procedure. The ISHLT consensus statement recommends against use as routine surveillance outside of clinical trials [52]. In addition to its value in research, IVUS may be of clinical value in selected patients in identifying the cause of unexplained graft failure (i.e., in the absence of rejection) patients with normal coronary arteriography.

Preventative Strategies on Coronary Artery Atherosclerotic Plaque Dimensions and Composition

Coronary artery disease continues to be the most common cause of mortality and morbidity worldwide and preventative strategies only reduce cardiovascular risk by 30–40 %. Germane to further reduction in cardiovascular risk are therapies directed at prevention of atherosclerotic disease. As described above, IVUS is able to detect the contours of the leading edge of the lumen and the media–adventitia interface and so permits direct measurements of the lumen and the total vessel cross-sectional area and absolute and percent plaque volume. While the relationship between low-density lipoprotein (LDL) cholesterol levels and coronary atherosclerosis was established in postmortem studies. The linear relationship between the LDL cholesterol levels and the atheroma plaque progression was first noted using IVUS [53, 54]. There have now been many studies that have studied the progression or regression of coronary atherosclerosis using IVUS. The REVERSAL (Reversal of Atherosclerosis with Aggressive Lipid Lowering) trial tested in a prospective, randomized manner the effect of 18 months of intensive versus moderate intensity lipid-lowering therapy on coronary artery plaque progression [55]. The intensive lipid-lowering arm reduced the LDL cholesterol levels to 78 mg/dL and stopped pro-

gression of atherosclerosis. The ASTERIOD (Study to Evaluate the Effect of Rosuvastatin on Intravascular Ultrasound-Derived Coronary Atheroma Burden) trial extended this observation by showing regression of atherosclerotic plaque volume with the use of high-intensity statin therapy [56]. Besides statins, other novel agents including inhibitors of acyl-coenzyme-A cholesterol acyltransferase (ACAT) and cholesterol ester transfer protein have been studied and these have shown no change in coronary plaque progression [57, 58].

Optical Coherence Tomography

OCT is a light-based imaging modality that generated high-resolution cross-sectional image of tissue microstructure [59]. Thus, the principle of OCT is similar to the use of ultrasound in IVUS. In essence, by measurement of the time delay of the optical echoes obtained due to reflection or backscatter from biological tissues, structural information as a function of depth can be obtained.

OCT light is in the near-infrared (NIR) range with wavelengths in the 1.3 μm . Both the bandwidth of the infrared light used and the wave velocity are orders of magnitude higher than in medical ultrasound. Like IVUS, the OCT image quality is dependent on the spatial resolution (distance between two points that are detectable by the imaging modality). This is measured as the degree of axial (line parallel to the light beam) or lateral resolution (perpendicular to the light beam) and is dependent on the spectral wavelength. Near the tip of the catheter, light is focused and directed at the vessel wall and as such the lateral resolution is best at its area. The resulting resolution is one order of magnitude larger than that of IVUS: the axial resolution of OCT is about 15 μm ; the lateral resolution is approximately 25 μm seen in Fig. 2.1 and Table 2.1. However, the imaging depth of approximately 1.0–1.5 mm within the coronary artery wall is less than that of IVUS.

OCT measures the time delay of light reflected or backscattered from tissue using interferometry. Light from the OCT system is split into a sample (going to the patient) and reference (going to a predetermined reference distance) segment.

Table 2.1 A comparison of FD-OCT and IVUS

| Variables | IVUS | FD-OCT |
|--------------------|--------------------|--|
| Wavelength | 1.3μ | 20–40 MHz |
| Resolution | 12–15 μm (axial) | 35–80 μm |
| | 20–40 μm (lateral) | 100–200 μm (axial) 200–300 μm (lateral) |
| Frame rate | 100 frames/s | 30 frames/s |
| Pullback rate | 20 mm/s | 0.5–1 mm/s |
| Max. scan diameter | 9.7 mm | 15 mm |
| Tissue penetration | 1.0–2.5 mm | 10 mm |

When light is reflected back from tissue, it is collected by the catheter, and combined. The distances between the sample and reference light transferred and detected generates a pattern of high and low intensities known as interference. The OCT system is able to interpret this pattern and determine the degree of backscatter in relation to depth. When the optics are rotated in the catheter around a 360° plane, the result is a cross-sectional image of the vessel wall.

There are two types of OCT systems: earlier time-domain OCT (TD-OCT) and recent Fourier-domain OCT (FD-OCT). In the FD-OCT system,

the depth profile can be constructed by the Fourier transform. Most signals can be thought of as a summation of sine waves with different frequencies. The Fourier transform extracts those frequencies, and their relative weights, from the signal. The source wavelength in Fourier-domain OCT can be swept at a much higher rate than the position scan of the reference arm mirror in a time-domain OCT system. This development has led to faster image acquisition speeds, with greater penetration depth, without loss of vital detail or resolution, and represents a great advancement on current conventional OCT systems [60]. Coronary arteries can be imaged with high OCT catheter pullback speeds within seconds, which allows for widespread clinical use in a broad range of patients and lesions.

**Optical Coherence Tomography:
Imaging Catheters and Imaging
Procedures**

OCT imaging catheters have an imaging core at the distal tip that is oriented at 90° to the length of the catheter as shown in Fig. 2.2. When these catheters are rotated along the long axis of the vessel a cross-

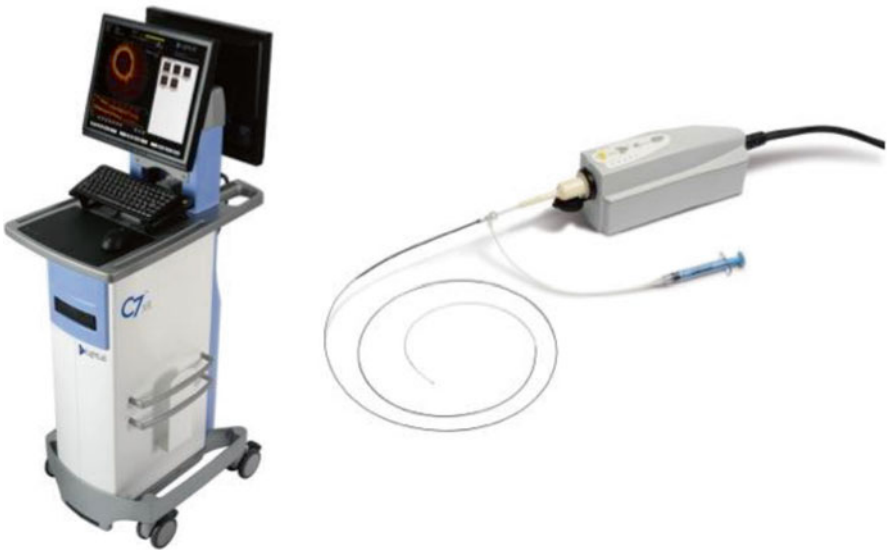


Fig. 2.2 Optical coherence tomography system (C7-XR) showing the image display on the *left* and the Dragonfly imaging catheter on the *right*. The Dragonfly catheter has

an insertable length of 135 cm with a 2.7 Fr tip and a 0.014 in. wire lumen and is able to produce images at 30 cm/s with a maximal length per run of 54 mm

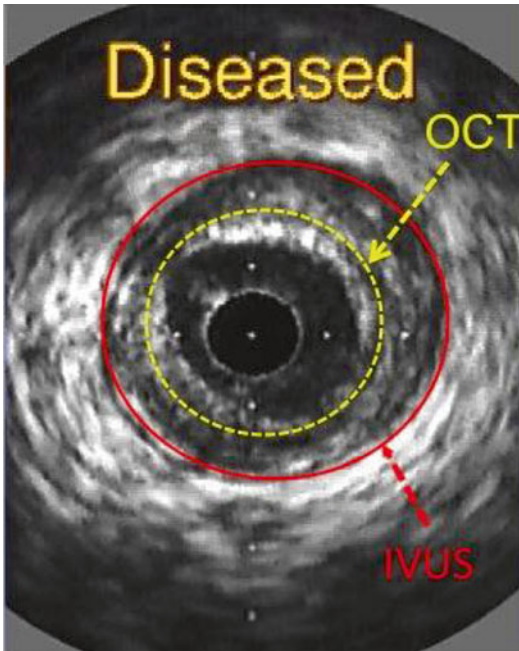


Fig. 2.3 Intravascular ultrasound (IVUS) cross-sectional image of a coronary arterial wall showing the imaging depth obtained by both modalities. *OCT* optical coherence tomography

sectional view of the coronary artery is obtained allowing the user to get a high-resolution image of the coronary artery. When performing an intracoronary OCT, the imaging catheter (2.7 Fr) is introduced over a guidewire (0.014 in.) into the distal coronary artery. A motorized pullback is performed to scan the coronary artery segment. The pullback speed is typically 20 mm/s with a frame rate of 100 frames per second or higher. Since blood scatters the OCT signal, it is temporarily cleared by an injection of X-ray contrast medium during the duration of the OCT pullback (typical flush rate 3.0 mL/s). A variety of solutions, warmed to 37 °C have been used alternatively as flush medium, including Lactated Ringer's, viscous iso-osmolar contrast media, and mixtures of lactated Ringer's and contrast media or low molecular weight dextrose. The time needed to image a 50 mm artery segment is typically 3 s with a total volume of X-ray contrast of 10–12 ml, which is comparable to the amount of X-ray contrast needed for a single angiographic run.

Like IVUS, current practice requires that patients be anticoagulated, typically with hepa-

rin, before insertion of the guidewire into the coronary artery. The image acquisition should be performed only after the administration of intracoronary nitroglycerin. In patients with severe left ventricular dysfunction, single remaining coronary vessel, renal dysfunction, and compromised hemodynamics, OCT should be performed with caution. In lesions with coexisting rich collateral blood flow or when coaxial positioning of the guiding catheter is not feasible, OCT imaging can be difficult due to the inability of blood clearance. In these cases, wire-based OCT can be used with a proximal balloon occlusion to facilitate blood clearance. If there are near complete stenosis or complete total occlusions of vessels, then OCT cannot be performed until there is antegrade restoration of blood flow.

OCT is a safe procedure with little applied energy (output power 5–8 mW) and is not thought to cause any functional or structural damage to tissue. The principle safety considerations relate to the possible induction of ischemia due to the need of blood displacement for image acquisition. This was more so with the TD-OCT systems where there was transient T-wave inversion or ST segment depression in 44–46 %, 1.1 % incidence of ventricular fibrillation, and 0.2 % risk of vessel dissection. Current OCT systems allow for very fast data within a few seconds and therefore are unlikely to lead to significant ischemia. In preliminary registries of patients imaged with FD-OCT, the most frequent event was transient T-wave inversion or ST segment depression (10 %) but there were no complications within a 24-h period [61, 62].

Components of the OCT Image

The normal vessel wall is characterized by layered architecture, comprising highly backscattered (signal-rich) intima (appears bright), followed by low backscattered (signal-poor media) and then heterogeneous but highly backscattered (signal-rich) adventitia as shown in Fig. 2.4. Light is highly reflected by the elastic membranes and this serves to distinguish between the three concentric layers with the innermost signal-rich layer reflects the internal elastic membrane and the

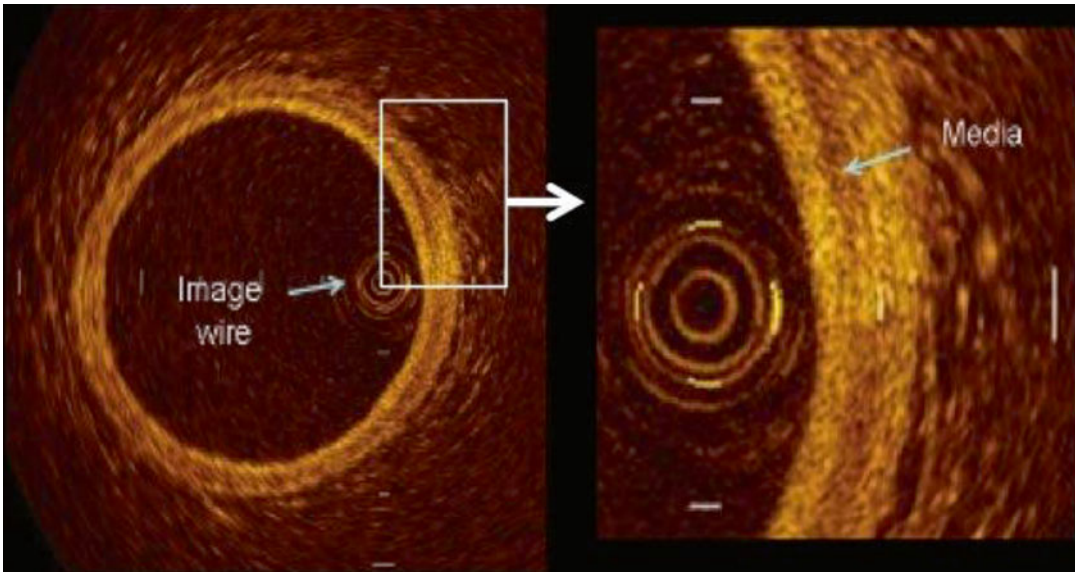


Fig.2.4 Optical coherence tomographic image of a normal coronary artery showing the cross-sectional anatomy. The normal vessel wall is characterized by layered architecture, comprising highly backscattered (signal-rich) intima

(appears bright), followed by low backscattered (signal-poor media) and then heterogeneous but highly backscattered (signal-rich) adventitia

outer, signal-rich layer representing the external elastic lamina. It must be noted that the normal three-layer appearance by OCT is not synonymous to the three-layer appearance by IVUS. IVUS cannot visualize the architecture of a normal coronary vessel due to its resolution of 120 μm while OCT is able to do so (resolution of 10 μm) as seen in Fig. 2.1.

IVUS and OCT images are fundamentally different from histology. However, owing to the high, 10 μm resolution of OCT, images do appear similar to histological sections. There may be some capacity to detect and quantify specific contents of vessel walls analogous to histological features. Caution must be used as not all features can be identified and the extent to which OCT can describe pathology is still unknown.

Qualitative Description of Atherosclerosis

As various components of atherosclerotic plaques have different optical properties, OCT makes it possible to differentiate between them.

The identification of plaque components by OCT depends on the degree of vessel wall penetration by the incident light beam. The depth of penetration is highest in fibrous tissues but least in thrombi with calcium and lipid tissue having intermediate values. There are distinct morphological characteristics that have been found when assessing atherosclerotic plaque.

- TCFA is a delineated necrotic core with an overlying fibrous cap where the minimal thickness of the fibrous cap is less than 65 μm (defined by histology) shown in Fig. 2.5. Thin fibrous cap atheromas are considered the most important morphologic substrate for a plaque at high risk to rupture and causing acute coronary syndrome. OCT allows the diagnosis of thin fibrous cap atheroma with a sensitivity of 90 % and a specificity of 79 % when compared to histopathology and for accurate measurement of the fibrous cap thickness with low variability [63]. Ongoing research suggests that the ability of OCT to measure changes in the fibrous cap thickness could be used to monitor the effect of therapeutic agents aiming at plaque stabilization although this is still extremely controversial.

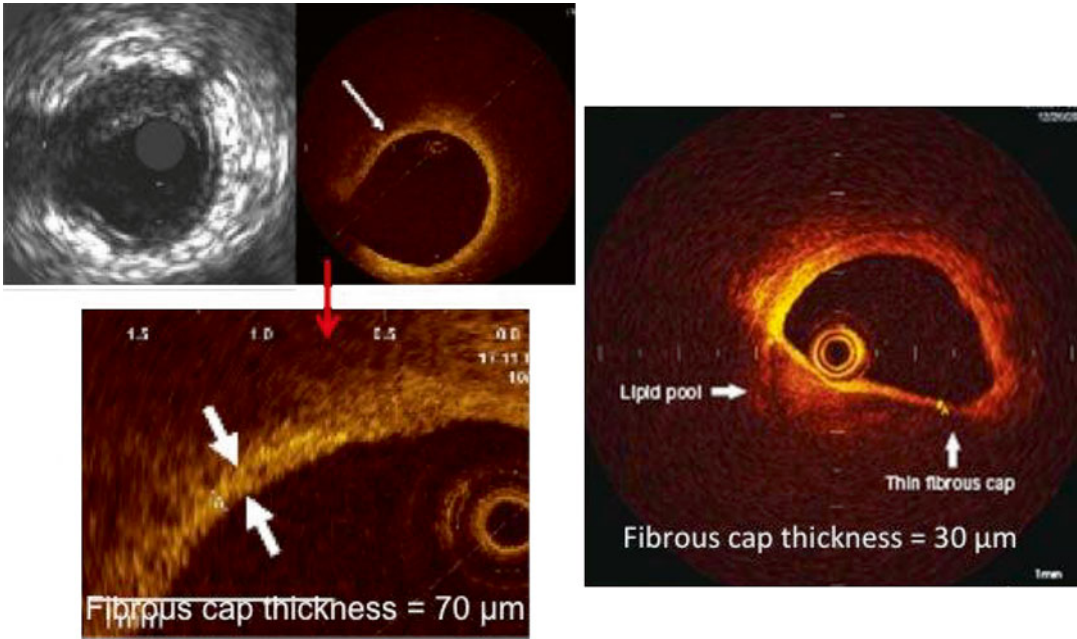


Fig. 2.5 Optical coherence tomographic images showing precise measurement of the fibrous cap thickness. The OCT image on the right shows a fibrous cap thickness of

<65 μm with a large lipid pool and is called a thin-cap fibroatheroma (TCFA)

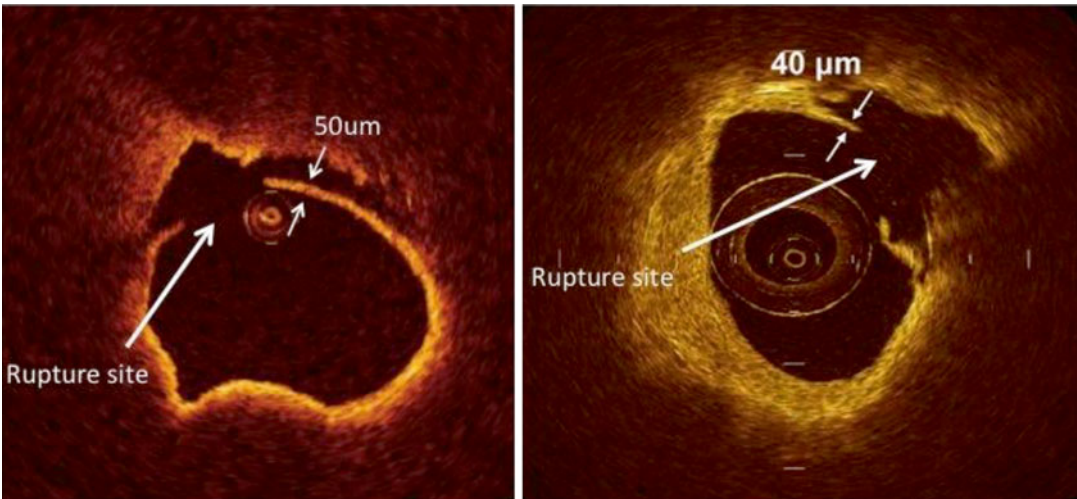


Fig. 2.6 Optical coherence tomographic image showing discontinuity of the fibrous cap with cavity formation in the plaque consistent with plaque rupture

- Atherosclerotic plaque (atheroma), which is a mass lesion (focal thickening) or loss of the layer structure of the vessel wall.
- Fibrous plaques have high backscattering with relatively homogenous signal due to the rich collagen or smooth muscle cells present in Fig. 2.6. Calcifications within plaques are identified by the

presence of well delineated, low backscattering, signal-poor heterogeneous regions.

- A necrotic core is a signal-poor region within an atherosclerotic plaque and has poorly defined borders often with overlying signal-rich bands, corresponding to fibrous caps. The necrotic core may also contain cholesterol

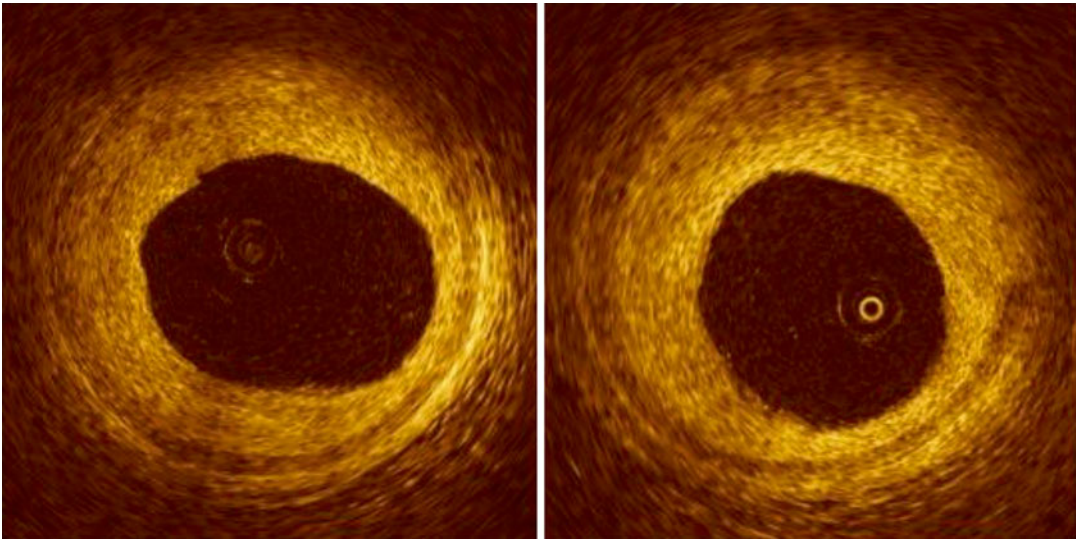


Fig. 2.7 Optical coherence tomographic image showing lipid plaque which is characterized by the regions of low reflectivity, diffuse margins, and high attenuation that appear homogenous

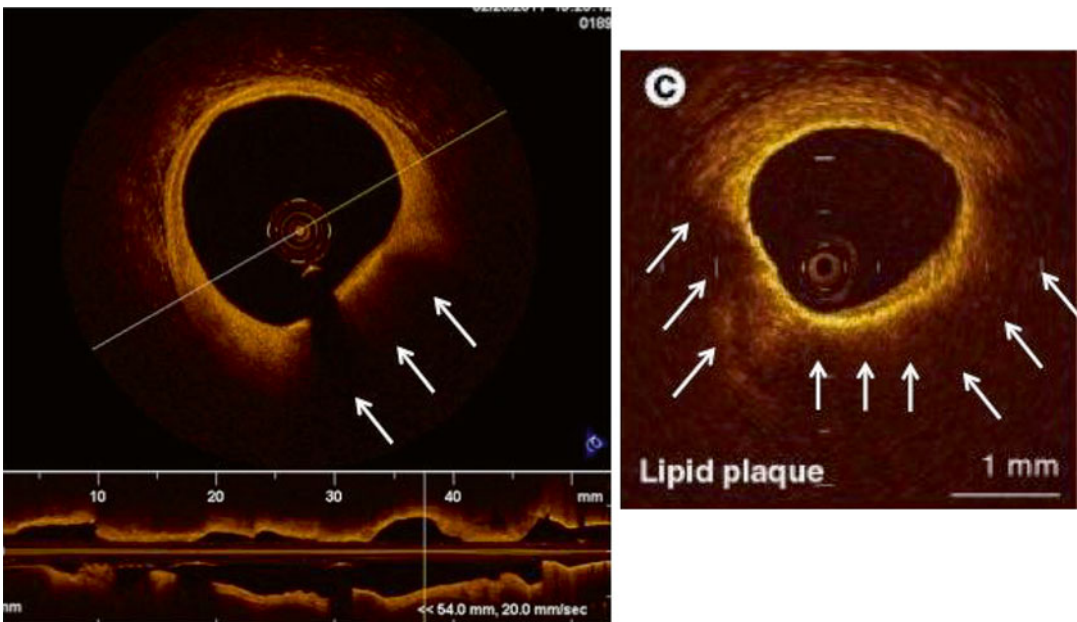


Fig. 2.8 Optical coherence tomographic image showing calcified plaque which is characterized by the regions of low reflectivity, sharp margins, and low attenuation that appear heterogenous

crystals (these appear as thin, linear region of high intensity). It is important to distinguish between the signal-poor regions noted due to the presence of calcium as shown in Fig. 2.7, which have sharply delineated signal-poor regions, as opposed to signal-poor regions of necrotic core, which are undefined or poorly

defined as shown in Fig. 2.8. The superiority of OCT for lipid-rich plaque detection has been confirmed in other studies comparing OCT-, IVUS-, and IVUS-derived techniques for plaque composition analysis

- Thrombi are identified as masses protruding into the vessel lumen discontinuous from the

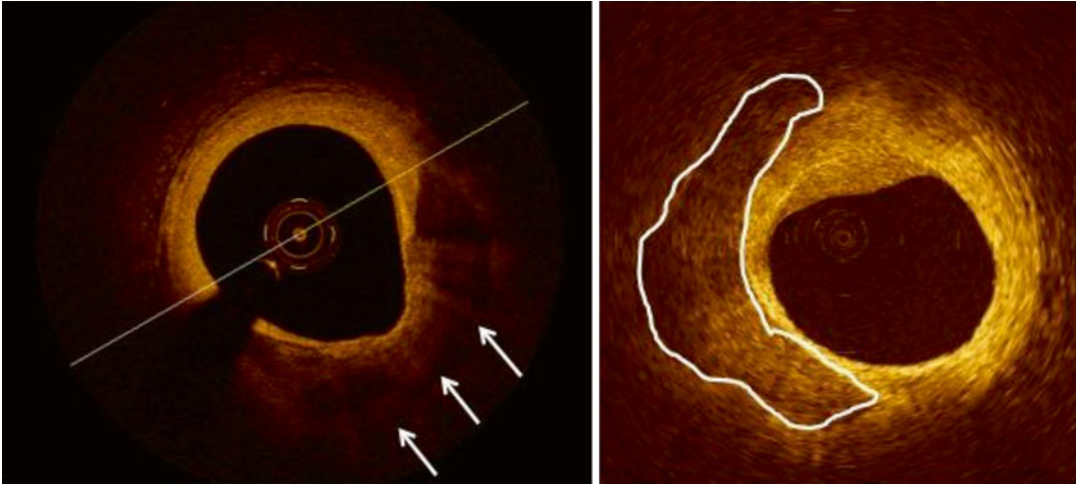


Fig. 2.9 Optical coherence tomographic image showing intracoronary thrombus. Red thrombi consist mainly of red blood cells; relevant OCT images are characterized as high-backscattering protrusions with signal-free shadow-

ing (seen on the *left*). White thrombi consist mainly of platelets and white blood cells and are characterized by a signal-rich, low-backscattering billowing projections protruding into the lumen (seen on the *right*)

surface of the vessel wall. Red thrombi consist mainly of red blood cells; relevant OCT images are characterized as high-backscattering protrusions with signal-free shadowing. White thrombi consist mainly of platelets and white blood cells and are characterized by a signal-rich, low-backscattering billowing projections protruding into the lumen as shown in Figs. 2.9 and 2.10. OCT is highly sensitive in diagnosing intracoronary thrombi, as the high contrast between the lumen and the surrounding structures facilitate the diagnosis. This is in contrast to IVUS where it is often difficult to differentiate thrombi from the blood-filled lumen or at times from soft plaque [64].

- Macrophage accumulation and intimal vasculature characterization have been described but are currently under investigation [65].

OCT in Plaque Rupture and Intracoronary Thrombosis

Acute coronary syndromes occur due to rupture of a coronary plaque triggering intracoronary thrombosis. Detecting lesions that are at high risk

for rupture may play a role in the prevention of future acute coronary syndromes. OCT has a unique role in the identification of lesions in unstable angina and specifically locates TCFA, which have ruptured or ulcerated. OCT allows for the diagnosis of TCFA with a sensitivity of 90 % and a specificity of 79 % when compared to histopathology [66]. In a study comparing OCT to IVUS and angiography in patients with myocardial infarction, OCT was able to estimate fibrous cap thickness [67]. Given the near-field resolution, OCT is well suited for in vivo detection of TCFA, follow the phenotype and assess for rupture. These applications provide the opportunity to assess the dynamic nature of atherosclerotic plaque and note changes over time. In fact, polarization-sensitive OCT (PS-OCT) is a new technology that can enhance OCT imaging using tissue birefringence allowing for the presence of collagen in vessel walls. This can be used to assess for the amount of collagen present in the TCFA allowing for an assessment of mechanical stability [68]. OCT is also ideally suited for the visualization of vessel morphology in the context of plaque rupture as the intima can be interrogated for an intimal tear, erosion, ulceration, or dissection of the TCFA and thrombus.

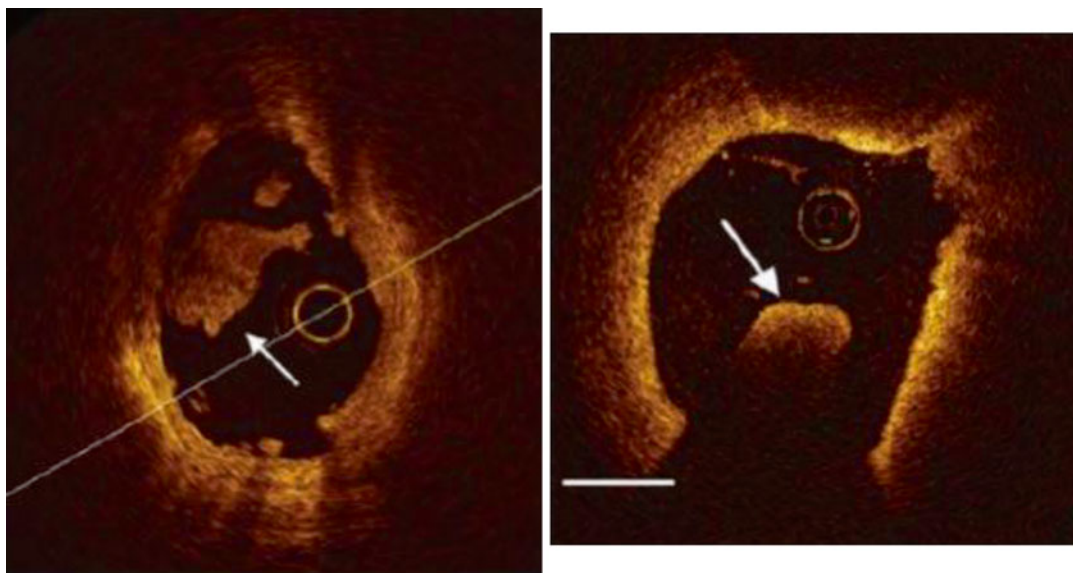


Fig. 2.10 Optical coherence tomographic image showing a fibrous plaque which is homogenous with high reflectivity, diffuse margins with less attenuation

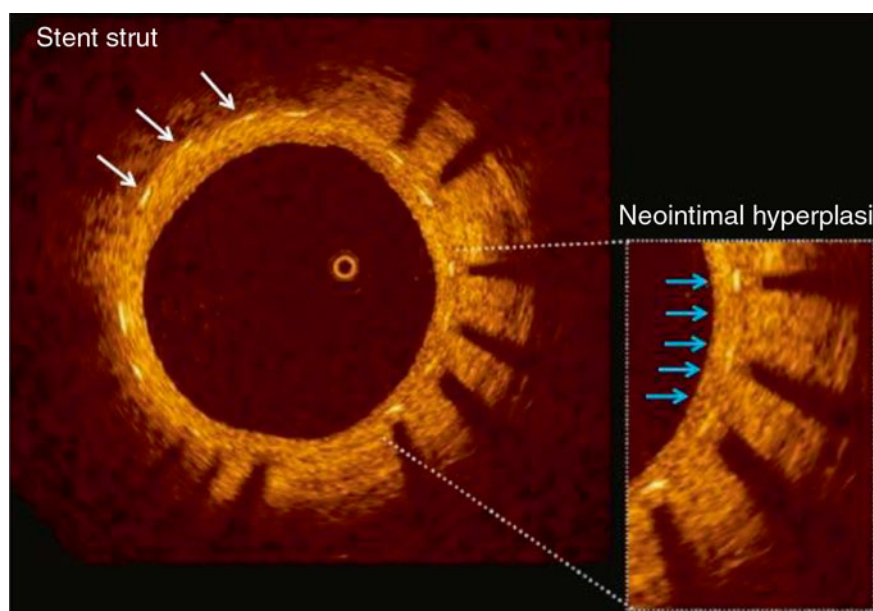


Fig. 2.11 Optical coherence tomographic image of neointimal coverage of a stent strut

OCT and the Assessment of Coronary Stents

IVUS has been used to assess the acute result following coronary stent implantation to assess for adequate stent expansion and apposition against

the wall seen in Fig. 2.11. The high-resolution capabilities of OCT and its diminished susceptibility to artifacts at the stent-strut surface compared to IVUS make it capable of visualizing tissue overlying the struts. These allow for precise determination if the struts are *covered* (tissue identified above the struts) or *uncovered*

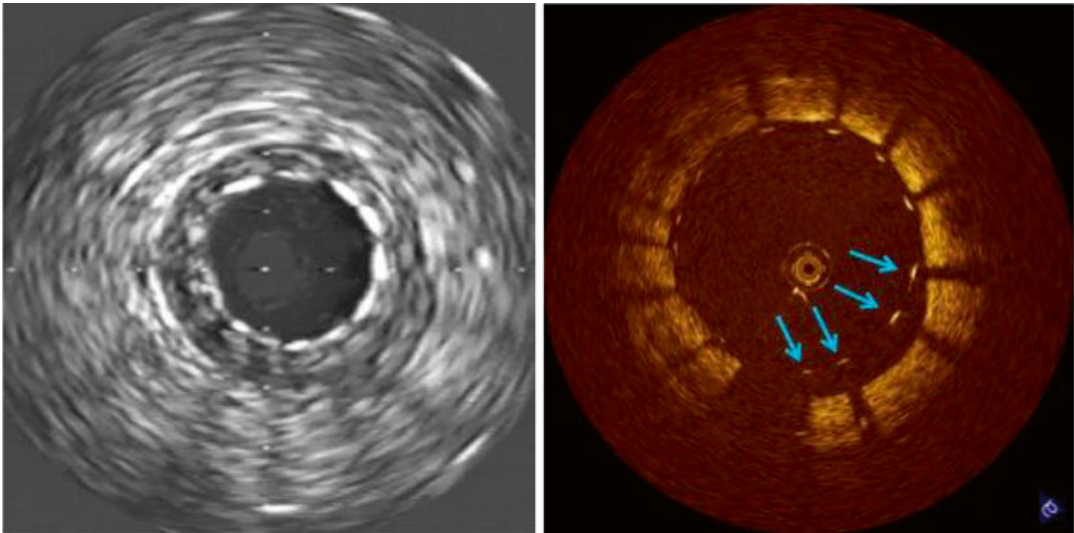


Fig. 2.12 A side by side comparison of an intravascular ultrasound image and optical coherence tomographic image of an intracoronary stent showing the superior resolution at detecting stent malapposition

(intervening space between the struts and the vessel wall) shown in Fig. 2.12. From a clinical viewpoint, a stent should be expanded with all struts apposed to the vessel wall (*covered*) in order to allow for optimal blood flow. IVUS studies have suggested that stent-strut malapposition is a relatively uncommon finding, observed in about 7 % of cases, and it does not increase the incidence of MACE [69, 70]. In contrast, OCT studies have demonstrated a high degree of struts (9.1 ± 7.4 % per lesion) that are not opposed to the wall and this is related to the strut thickness, closed cell design, overlapping nature of the stents, and acute stent recoil [66]. In cases of malapposition of stents, a high pressure deployment is performed but this can result in peri-procedural vessel damage. OCT is able to determine the degree of vessel damage and also characterize the presence and nature of disease in the segments proximal and distal to the stented segments [67]. Plaque type (TCFA versus fibrous) at the proximal and distal edge of the stents are important determinants of the incidence of edge dissection [71]. While the observations are useful for better design and deployment of stents, the clinical relevance is currently unknown.

Long-term stent-strut/vessel wall interaction is of interest to both researchers and clinicians.

The stability of the acute result, the identification of complex anatomy that is not accessible by angiography or IVUS, and the understanding of reasons for stent failures, when they do occur, are example of information that is of interest. In contrast to IVUS, OCT can reliably detect and quantify early and very thin layers of tissue coverage on stent struts [72–74], even in DES with very thin layers of neointima, often below 80 μm in thickness, with high reliability.

OCT has been employed in prospective clinical trials to compare the long-term outcome of various stents:

- The LEADERS randomized trial was a comparison of a biolimus-eluting stent (BES) with biodegradable polymer with sirolimus-eluting stent using a durable polymer. Fifty-six consecutive patients underwent OCT during angiographic follow-up at 9 months. Strut coverage at an average follow-up of 9 months was significantly more complete in patients allocated to BES when compared to those with SES [weighted difference -1.4 %, 95 % CI, -3.7 to 0.0] [75]
- In the Harmonizing Outcomes with Revascularization and Stents in Acute Myocardial Infarction (HORIZONS-AMI) trial, patients with STEMI were randomized to

paclitaxel-eluting stent (PES) or BMS implantation. The OCT substudy revealed that implantation of PES as compared with BMS significantly reduced neointimal hyperplasia but resulted in higher rates of uncovered and malapposed stent struts at 13-month follow-up ($1.1 \pm 2.5\%$ in BMS lesions versus $5.7 \pm 7.0\%$ in PES lesions) [76].

- OCT was employed to study tissue coverage at follow-up in bioresorbable scaffolds. OCT was able to visualize the particular structure of the scaffold struts, the tissue coverage over time, as well as the changes in the optical properties of the vascular tissue during the bioresorption process [77].

While these observations are important to understand differences in-stent design, further studies are required to determine the clinical significance of these findings. Today, no threshold for coverage is established. Pathological data in humans suggest that neointimal coverage of stent struts could be used as a surrogate for endothelialization due to the good correlation between strut coverage and thrombus formation. However, OCT data must be interpreted with caution as OCT resolution will still miss a single layer of endothelial cells over struts and the presence of an OCT detectable endothelial layer does not imply a functional endothelium. Despite these limitations, OCT is the only imaging modality to date that offers the possibility to understand tissue coverage and neointimal formation in intracoronary stents.

Other Clinical Applications of OCT

Today, no clinical indications for OCT imaging are established. There are no randomized data supporting a prognostic role for OCT in catheter-based intervention. However, there is broad expert agreement that the detailed, easy accessible and interpretable information of OCT on the presence of atherosclerosis, its extent, lumen narrowing as well as on the result of any interventional measure can be of clinical value, at least in individual patients and in specific clinical scenarios

Conclusion

Intracoronary imaging has resulted in significant gains in our understanding of the nature of atherosclerosis and vessel biology. OCT has added to this by the generation of unprecedented image resolution and its application for the visualization of atherosclerotic plaques, stents, and the stent–vessel interaction is an exciting area of current investigation.

References

1. Brown MS, Goldstein JL. Heart attacks: gone with the century? *Science*. 1996;272:629.
2. Glagov S, Weisenberg E, Zarins CK. Compensatory Enlargement of Human Atherosclerotic Coronary Arteries. *N Engl J Med*. 1987;316:1371–5.
3. von Birgelen C, Slager CJ, Di Mario C, de Feyter PJ, Serruys PW. Volumetric intracoronary ultrasound: a new maximum confidence approach for the quantitative assessment of progression-regression of atherosclerosis? *Atherosclerosis*. 1995;118(Suppl):S103–13.
4. Böse D, von Birgelen C, Erbel R. Intravascular ultrasound for the evaluation of therapies targeting coronary atherosclerosis. *J Am Coll Cardiol*. 2007;49:925–32.
5. Mintz GS, Nissen SE, Anderson WD, Bailey SR, Erbel R, Fitzgerald PJ, et al. American College of Cardiology clinical expert consensus document on standards for acquisition, measurement and reporting of intravascular ultrasound studies. *J Am Coll Cardiol*. 2001;37:1478–92.
6. Di Mario C, Görges G, Peters R, Kearney P, Pinto F, Hausmann D, et al. Clinical application and image interpretation in intracoronary ultrasound. *Eur Heart J*. 1998;19:207–29.
7. von Birgelen C, de Very EA, Mintz GS, Nicosia A, Bruining N, Li W, et al. ECG-gated three-dimensional intravascular ultrasound: feasibility and reproducibility of the automated analysis of coronary lumen and atherosclerotic plaque dimensions in humans. *Circulation*. 1997;96:2944–52.
8. Jensen LO, Thayssen P, Pedersen KE, Stender S, Haghfelt T. Low variation and high reproducibility in plaque volume with intravascular ultrasound. *Int J Cardiol*. 2004;97:463–9.
9. Kastelein JJ, de Groot E. Ultrasound imaging techniques for the evaluation of cardiovascular therapies. *Eur Heart J*. 2008;29:849–58.
10. Lindsay AC, Choudhury RP. Form to function: current and future roles for atherosclerosis imaging in drug development. *Nat Rev Drug Discov*. 2008;7:517–29.

11. Low AF, Kawase Y, Chan YH, Tearney GJ. In vivo characterization of coronary plaques with conventional grey-scale intravascular ultrasound: correlation with optical coherence tomography. *EuroIntervention*. 2009;4:626–32.
12. Okubo M, Kawasaki M, Ishihara Y. Tissue characterization of coronary plaques: comparison of integrated backscatter intravascular ultrasound with virtual histology intravascular ultrasound. *Circulation*. 2008;72:1631–9.
13. Nair A, Kuban BD, Tuzcu EM. Coronary plaque classification with intravascular ultrasound radiofrequency data analysis. *Circulation*. 2002;106:2200–6.
14. Kawasaki M, Bouma BE, Bresser J. Diagnostic accuracy of optical coherence tomography and integrated backscatter intravascular ultrasound images for tissue characterization of human coronary plaques. *J Am Coll Cardiol*. 2006;45:1946–53.
15. Cespedes EI, de Korte CL, van der Steen AF. Intraluminal ultrasonic palpation: assessment of local and cross-sectional tissue stiffness. *Ultrasound Med Biol*. 2000;26:385–96.
16. Doyle MM, Mastik F, de Korte CL. Advancing intravascular ultrasonic palpation towards clinical applications. *Ultrasound Med Biol*. 2001;27:1471–80.
17. Sheifer SE, Canos MR, Weinfurt KP. Sex differences in coronary artery size assessed by intravascular ultrasound. *Am Heart J*. 2000;139:649.
18. Herity NA, Lo S, Lee DP. Effect of a change in gender on coronary arterial size: a longitudinal ultrasound study in transplanted hearts. *J Am Coll Cardiol*. 2003;41:1539.
19. Mintz GS, Popma JJ, Pichard AD. Limitations of angiography in the assessment of plaque distribution in coronary artery disease: a systemic study of target lesion eccentricity in 1446 lesions. *Circulation*. 1996;93:924.
20. Ziada KM, Tuzcu EM, De Franco AC. Intravascular ultrasound assessment of the prevalence and causes of angiographic “haziness” following high-pressure coronary stenting. *Am J Cardiol*. 1997;80:116.
21. Mintz GS, Painter JA, Pichard AD, et al. Atherosclerosis in angiographically “normal” coronary artery reference segments: an intravascular ultrasound study with clinical correlations. *J Am Coll Cardiol*. 1995;25:1479.
22. St Goar FG, Pinto FJ, Alderman EL, et al. Intravascular ultrasound imaging of angiographically normal coronary arteries: an in vivo comparison with quantitative angiography. *J Am Coll Cardiol*. 1991;18:952.
23. Glagov S, Weisenberg E, Zarins CK, et al. Compensatory enlargement of human atherosclerotic coronary arteries. *N Engl J Med*. 1987;316:1371.
24. Ziada KM, Tuzcu EM, De Franco AC. Intravascular ultrasound assessment of the prevalence and causes of angiographic “haziness” following high-pressure coronary stenting. *Am J Cardiol*. 1997;80:116–21.
25. Bech GL, De Bruyne B, Pijls NH. Fractional flow reserve to determine the appropriateness of angioplasty in moderate coronary stenosis: a randomized trial. *Circulation*. 2001;103:2928–34.
26. Briguori C, Anzuini A, Airolidi F. Intravascular ultrasound criteria for the assessment of functional significance of intermediate coronary artery stenosis and comparison with functional flow reserve. *Am J Cardiol*. 2001;87:136–41.
27. Ricciardi MJ, Meyers S, Choi K, Pang J. Angiographically silent left main disease detected by intravascular ultrasound: a marker for future adverse cardiac events. *Am Heart J*. 2003;146:507–12.
28. Kang SJ, Lee JY, Ahn JM. Intravascular ultrasound derived predictors for fractional flow reserve in intermediate left main disease. *J Am Coll Cardiol Interv*. 2011;4:1168–74.
29. Timmis SB, Burns WJ, Hermiller JB, et al. Influence of coronary atherosclerotic remodeling on the mechanism of balloon angioplasty. *Am Heart J*. 1997;134:1099.
30. Smith Jr SC, Feldman TE, Hirshfeld Jr JW, et al. ACC/AHA/SCAI 2005 guideline update for percutaneous coronary intervention—summary article: a report of the American College of Cardiology/American Heart Association Task Force on Practice Guidelines (ACC/AHA/SCAI Writing Committee to Update 2001 Guidelines for Percutaneous Coronary Intervention). *J Am Coll Cardiol*. 2006;47:216–35.
31. Cutlip DE, Baim DS, Ho KK, et al. Stent thrombosis in the modern era: a pooled analysis of multicenter coronary stent clinical trials. *Circulation*. 2001;103:1967–71.
32. Cheneau E, Leborgne L, Mintz GS, et al. Predictors of subacute stent thrombosis: results of a systematic intravascular ultrasound study. *Circulation*. 2003;108:43–7.
33. Fitzgerald PJ, Oshima A, Hayase M, et al. Final results of the Can Routine Ultrasound Influence Stent Expansion (CRUISE) study. *Circulation*. 2000;102:523–30.
34. Uren NG, Schwarzacher SP, Metz JA, et al. for the POST Registry Investigators. Predictors and outcomes of stent thrombosis: an intra-vascular ultrasound registry. *Eur Heart J*. 2002;23:124–32.
35. Doi H, Maehara A, Mintz GS, et al. Impact of post-intervention minimal stent area on 9-month follow-up patency of paclitaxel-eluting stents: an integrated intravascular ultrasound analysis from the TAXUS IV, V, and VI and TAXUS ATLAS Workhorse, Long Lesion, and Direct Stent Trials. *J Am Coll Cardiol Interv*. 2009;2:1269–75, 27.
36. Eshtehardi P, Samady H. Intravascular ultrasound for assessment of coronary drug-eluting stent deployment: an evolving field in need of new criteria. *J Am Coll Cardiol Interv*. 2010;3:364.
37. Kasaoka S, Tobis JM, Akiyama T, et al. Angiographic and intravascular ultrasound predictors of in-stent restenosis. *J Am Coll Cardiol*. 1998;32:1630–5.
38. Parise H, Maehara A, Stone GW, Leon MB, Mintz GS. Meta-analysis of randomized studies comparing intravascular ultrasound versus angiographic guidance of percutaneous coronary intervention in pre-drug-eluting stent era. *Am J Cardiol*. 2011;107:374–82.

39. Park SM, Kim JS, Ko YG, et al. Angiographic and intravascular ultrasound follow up of paclitaxel- and sirolimus-eluting stent after poststent high-pressure balloon dilation: from the poststent optimal stent expansion trial. *Catheter Cardiovasc Interv.* 2011; 77:15–21.
40. Jakabcin J, Spacek R, Bystron M, et al. Long-term health outcome and mortality evaluation after invasive coronary treatment using drug eluting stents with or without the IVUS guidance. Randomized control trial. HOME DES IVUS. *Catheter Cardiovasc Interv.* 2010;75:578–83.
41. Colombo A, Caussin C, Presbitero P, et al. AVIO: A prospective, randomized trial of intravascular-ultrasound guided compared to angiography guided stent implantation in complex coronary lesions (abstr). *J Am Coll Cardiol* 2010;56:Suppl B:xvii.
42. Roy P, Steinberg DH, Sushinsky SJ, et al. The potential clinical utility of intravascular ultrasound guidance in patients undergoing percutaneous coronary intervention with drug-eluting stents. *Eur Heart J.* 2008;29:1851–7.
43. Choi SY, Witzembichler B, Maehara A, et al. Intravascular ultrasound findings of early stent thrombosis after primary percutaneous intervention in acute myocardial infarction: a Harmonizing Outcomes with Revascularization and Stents in Acute Myocardial Infarction (HORIZONS-AMI) substudy. *Circ Cardiovasc Interv.* 2011;4:239–47.
44. Oemrawsingh PV, Mintz GS, Schali J MJ, et al. Intravascular ultrasound guidance improves angiographic and clinical outcome of stent implantation for long coronary artery stenoses: final results of a randomized comparison with angiographic guidance (TULIP Study). *Circulation.* 2003;107:62.
45. Park SJ, Kim YH, Park DW. Impact of intravascular ultrasound guidance on long-term mortality in stenting for unprotected left main coronary artery stenosis. *Circ Cardiovasc Interv.* 2009;28:1304–9.
46. Tuzcu EM, Kapadia SR, Sachar R, et al. Intravascular ultrasound evidence of angiographically silent progression in coronary atherosclerosis predicts long-term morbidity and mortality after cardiac transplantation. *J Am Coll Cardiol.* 2005;45:1538.
47. Mehra MR, Ventura HO, Stapleton DD, et al. Presence of severe intimal thickening by intravascular ultrasonography predicts cardiac events in cardiac allograft vasculopathy. *J Heart Lung Transplant.* 1995;14:632.
48. Kapadia SR, Nissen SE, Ziada KM, et al. Development of transplantation vasculopathy and progression of donor-transmitted atherosclerosis: comparison by serial intravascular ultrasound imaging. *Circulation.* 1998;98:2672.
49. Barbir M, Lazem F, Banner N, et al. The prognostic significance of non-invasive cardiac tests in heart transplant recipients. *Eur Heart J.* 1997;18:692.
50. Kobashigawa JA, Tobis JM, Starling RC, et al. Multicenter intravascular ultrasound validation study among heart transplant recipients: outcomes after five years. *J Am Coll Cardiol.* 2005;45:1532.
51. Ramasubbu K, Schoenhagen P, Balghith MA, et al. Repeated intravascular ultrasound imaging in cardiac transplant recipients does not accelerate transplant coronary artery disease. *J Am Coll Cardiol.* 2003;41:1739.
52. Mehra MR, Crespo-Leiro MG, Dipchand A, et al. International Society for Heart and Lung Transplantation working formulation of a standardized nomenclature for cardiac allograft vasculopathy-2010. *J Heart Lung Transplant.* 2010;29:717.
53. von Birgelen C, Hartmann M, Mintz GS, Baumgart D, Schmermund A, Erbel R. Relation between progression and regression of atherosclerotic left main coronary artery disease and serum cholesterol levels as assessed with serial long-term (≥ 12 months) follow-up intravascular ultrasound. *Circulation.* 2003;108:2757–62.
54. Hartmann M, von Birgelen C, Mintz GS, van Houwelingen GK, Eggebrecht H, Boerse D et al. Relation between plaque progression and low-density lipoprotein cholesterol during aging as assessed with serial long-term (≥ 12 months) follow-up intravascular ultrasound of the left main coronary artery. *Am J Cardiol.* 2006;98:1419–23.
55. Nissen SE, Tuzcu EM, Schoenhagen P, Brown BG, Ganz P, Vogel RA, et al. Effect of intensive compared with moderate lipid-lowering therapy on progression of coronary atherosclerosis: a randomized controlled trial. *JAMA.* 2004;291:1071–80.
56. Nissen SE, Nicholls SJ, Sipahi I, Libby P, Raichlen JS, Ballantyne CM, et al. Effect of very high-intensity statin therapy on regression of coronary atherosclerosis: the ASTEROID trial. *JAMA.* 2006;295:1556–65.
57. Nissen SE, Tuzcu EM, Brewer HB, Sipahi I, Nicholls SJ, Ganz P, et al. Effect of ACAT inhibition on the progression of coronary atherosclerosis. *N Engl J Med.* 2006;354:1253–63.
58. Nissen SE, Tardif JC, Nicholls SJ, Revkin JH, Shear CL, Duggan WT, et al. Effect of torcetrapib on the progression of coronary atherosclerosis. *N Engl J Med.* 2007;356:1304–16.
59. Haug D, Swanson EA, Lin CP. Optical coherence tomography. *Science.* 1991;254:1178–81.
60. Takarada S, Imanishi T, Liu Y. Advantage of next-generation frequency-domain optical coherence tomography compared to conventional time-domain system in the assessment of coronary lesion. *Catheter Cardiovasc Interv.* 2010;75:202–6.
61. Barlis P, Gonzalo N, Di Mario C. A multicenter evaluation of the safety of intracoronary optical coherence tomography. *EuroIntervention.* 2009;5:90–5.
62. Imola F, Mallus MT, Ramazzotti V. Safety and feasibility of frequency domain optical coherence tomography to guide decision making in percutaneous coronary intervention. *EuroIntervention.* 2010;6:575–81.
63. Virmani R, Burke AP, Farb A. Pathology of the vulnerable plaque. *J Am Coll Cardiol.* 2006;47:C13–8.
64. Kume T, Akasaka T, Kawamoto T. Assessment of coronary arterial thrombus by optical coherence tomography. *Am J Cardiol.* 2006;97:1713–7.

65. Tearney GJ, Yabushita H, Houser SL, et al. Quantification of macrophage content in atherosclerotic plaques by optical coherence tomography. *Circulation*. 2003;107:113–9.
66. Kume T, Okura H, Yamada R, et al. Frequency and spatial distribution of thin-cap fibroatheroma assessed by 3-vessel intravascular ultrasound and optical coherence tomography: an ex vivo validation and an initial in vivo feasibility study. *Circ J*. 2009;73:1086–91.
67. Barlis P, Serruys PW, Gonzalo N, et al. Assessment of culprit and remote coronary narrowings using optical coherence tomography with long-term outcomes. *Am J Cardiol*. 2008;102:391–5.
68. Nadkarni SK, Pierce MC, Park BH, et al. Measurement of collagen and smooth muscle cell content in atherosclerotic plaques using polarization-sensitive optical coherence tomography. *J Am Coll Cardiol*. 2007;49:1474–81.
69. Hong MK, Mintz GS, Lee CW, et al. Late stent malapposition after drug-eluting stent implantation: an intravascular ultrasound analysis with long-term follow-up. *Circulation*. 2006;113:414–9.
70. Tanabe K, Serruys PW, Degertekin M, et al. Incomplete stent apposition after implantation of paclitaxel-eluting stents or bare metal stents: insights from the randomized TAXUS II trial. *Circulation*. 2005;111:900–5.
71. Bouma BE, Tearney GJ, Yabushita H, et al. Evaluation of intracoronary stenting by intravascular optical coherence tomography. *Heart*. 2003;89:317–20.
72. Tanigawa J, Barlis P, Dimopoulos K, Di Mario C. Optical coherence tomography to assess malapposition in overlapping drug-eluting stents. *EuroIntervention*. 2008;3:580–3.
73. Gonzalo N, Serruys PW, Okamura T, et al. Optical coherence tomography assessment of the acute effects of stent implantation on the vessel wall: a systematic quantitative approach. *Heart*. 2009;95:1913–9.
74. Tanimoto S, Rodriguez-Granillo G, Barlis P, et al. A novel approach for quantitative analysis of intracoronary optical coherence tomography: high interobserver agreement with computer-assisted contour detection. *Catheter Cardiovasc Interv*. 2008;72:228–35.
75. Barlis P, Regar E, Serruys PW, et al. An optical coherence tomography study of a biodegradable vs. durable polymer-coated limus-eluting stent: a LEADERS trial sub-study. *Eur Heart J*. 2010;31:165–76.
76. Guagliumi G, Costa MA, Sirbu V, et al. Strut coverage and late malapposition with paclitaxel-eluting stents compared with bare metal stents in acute myocardial infarction: optical coherence tomography substudy of the Harmonizing Outcomes with Revascularization and Stents in Acute Myocardial Infarction (HORIZONS-AMI) Trial. *Circulation*. 2011;123:274–81.
77. van Beusekom HM, Serruys PW. Drug-eluting stent endothelium: presence or dysfunction. *JACC Cardiovasc Interv*. 2011;3:76–7.

Imaging Coronary Atherosclerosis

Nicholls, S.J.; Crowe, T. (Eds.)

2014, XIII, 220 p. 81 illus., 71 illus. in color., Hardcover

ISBN: 978-1-4939-0571-3

A product of Humana Press